

Table V
Molecular Weights of PVC and E-V Copolymers

polymer	M_n		M_w		M_w/M_n
	obsd ^a	calcd ^b	obsd ^a	calcd ^b	
PVC	58 000		106 000		1.8
E-V-84	50 000	53 000	109 000	97 000	2.2
E-V-14	26 000	30 000	38 000	55 000	1.5

^a GPC. ^b Expected from chlorine loss.

discussion should be facilitated by comparison of the microstructures of additional E-V copolymers obtained both by Bu_3SnH and LiAlH_4 reduction and also by examining the products resulting from the reduction of PVC oligomers.

Table V presents the results of our GPC analyses of the molecular weights of our starting PVC and two E-V copolymers obtained by reductive dechlorination of PVC with Bu_3SnH . Comparison of the molecular weights expected from loss of chlorine with those measured by GPC for E-V-84 and E-V-14 indicate that Bu_3SnH reduction of PVC does not produce significant chain scission or cross-linking. Instead, our initial PVC containing a number average of ~ 1000 repeat units has been converted to a series of E-V copolymers each of ~ 1000 repeat units.

Reductive dechlorination of PVC with Bu_3SnH has produced a series of E-V copolymers each with the same chain length as the starting PVC, but with differing amounts of pendant chlorine atoms. Detailed ^{13}C NMR analysis, which was materially assisted by chemical shifts calculated⁸ by the γ -gauche effect method,¹⁴ has revealed the overall comonomer composition, comonomer sequence distribution, and the stereoregularity of the vinyl chloride sequences. Thus, we have a well-characterized copolymer system upon which we are proceeding to measure physical properties in the hope of eventually being able to establish structure-property relations.

Acknowledgment. We are indebted to M. Y. Hellman for performing GPC analyses, to W. H. Starnes, Jr., for providing 4,6-dichlorononane, and to R. E. Cais for a careful reading of this manuscript and for valuable discussions.

References and Notes

- (1) W. H. Starnes, Jr., F. C. Schilling, I. M. Plitz, R. E. Cais, D. J. Freed, R. C. Hartless, and F. A. Bovey, *Macromolecules* **16**, 790 (1983), and references cited therein.
- (2) A. E. Tonelli, F. C. Schilling, T. N. Bowmer, and M. Valenciano, *Polym. Prepr., Am. Chem. Soc., Div. Polym. Chem.*, **24**, 211 (1983).
- (3) R. E. Cais and J. M. Kometani, *Macromolecules*, **15**, 954 (1982).
- (4) F. Keller and C. Mugge, *Faserforsch. Textiltech.*, **27**, 347 (1976).
- (5) A. Misono, Y. Uchida, and K. Yamada *J. Polym. Sci., Part B*, **5**, 401 (1967); *Bull. Chem. Soc. Jpn.*, **40**, 2366 (1967).
- (6) A. Misono, Y. Uchida, K. Yamada, and T. Saeki, *Bull. Chem. Soc. Jpn.*, **41**, 2995 (1968).
- (7) M. Hagiwara, T. Miura, and T. Kagiya, *J. Polym. Sci., Part A-1*, **7**, 513 (1969).
- (8) A. E. Tonelli and F. C. Schilling, *Macromolecules*, **14**, 74 (1981).
- (9) G. Khanarian and A. E. Tonelli, *J. Chem. Phys.*, **25**, 5031 (1981); *Macromolecules*, **15**, 145 (1982); *ACS Symp. Ser. No. 233*, 235 (1983).
- (10) G. Khanarian, R. E. Cais, J. M. Kometani, and A. E. Tonelli, *Macromolecules*, **15**, 866 (1982).
- (11) G. Khanarian, F. C. Schilling, R. E. Cais, and A. E. Tonelli, *Macromolecules*, **16**, 287 (1983).
- (12) F. C. Schilling, *Macromolecules*, **11**, 1290 (1978).
- (13) F. C. Schilling, unpublished observations.
- (14) A. E. Tonelli and F. C. Schilling, *Acc. Chem. Res.*, **14**, 233 (1981).
- (15) R. E. Cais and N. J. A. Sloan, *Polymer*, **24**, 179 (1983).
- (16) J. C. Randall, "Polymer Sequence Determination", Academic Press, New York, 1977.
- (17) F. C. Schilling, unpublished observations on commercially obtained 2,4-dimethylpentane and 4,6-dimethylnonane synthesized and provided by W. H. Starnes, Jr., and co-workers.
- (18) W. H. Starnes, Jr., F. C. Schilling, K. B. Abbás, I. M. Plitz, R. C. Hartless, and F. A. Bovey, *Macromolecules*, **12**, 13 (1979).

Multinuclear Magnetic Relaxation Studies of Aqueous Poly(ethylene oxide) Solutions Containing Alkali Halides

Ebba Florin

Department of Physical Chemistry, The Royal Institute of Technology, S-100 44 Stockholm, Sweden. Received August 29, 1983

ABSTRACT: The nuclear magnetic relaxation rates of ^7Li , ^{23}Na , ^{133}Cs , ^{35}Cl , and ^{81}Br have been measured for alkali halide-poly(ethylene oxide) (PEO)-water mixtures. Addition of PEO to aqueous salt solutions increases the relaxation rates markedly for all the nuclei studied. The largest effect has been observed for ^{133}Cs : in a 1.0 *m* CsBr solution containing 45% PEO by weight its relaxation rate is ~ 65 times larger than that in the polymer-free solution. The increases found are mainly caused by (i) asymmetric hydration of the ions, induced by the PEO, and (ii) direct cation-ether oxygen interactions of the same type—but much weaker—as in metal complexes with crown ethers and similar compounds. From the temperature dependences of the relaxation rates activation energies have been calculated. Addition of PEO raises the activation energy—typically by a factor of ~ 4 for a PEO-rich sample compared to that of a pure aqueous salt solution—which reflects a stabilization of the water structure, due to the presence of the polymer.

Introduction

Solutions of poly(ethylene oxide) (PEO) have been investigated by NMR spectroscopy for a long time, as can be seen in the literature. Various NMR methods have been used and, accordingly, the spectroscopic results give

different pieces of information about the properties of the systems.

Most common are ^1H relaxation measurements on the methylene protons of PEO, which have, for instance, been made in different solvents and correlated to the solvent

viscosities.¹ It has also been shown that the T_1 values of the methylene protons depend neither on the degree of polymerization (for molecular weights above ~ 4000) nor very markedly on the concentration of PEO in aqueous solutions.² Self-diffusion coefficients for PEO in water and in organic solvents have been determined with the pulsed field gradient method.³ Studies of the chemical shifts of the methylene protons indicate that in aqueous solutions of the polymer an approximate number of water molecules (≈ 2) are needed for the chains to become fully hydrated.⁴ Further, from variations with temperature of the splittings in ^{13}C -H satellite sidebands of proton NMR spectra of PEO, it is concluded that the *gauche* conformations of the chain are predominant. This is shown to be valid for PEO in both water and chloroform.⁵ The correlation times obtained from ^{13}C and ^1H experiments as well as those from ESR measurements on spin-labeled PEO show that the polymer is highly flexible in organic solvents.⁶

The PEO-water phase diagram includes a solubility gap at elevated temperatures⁷ and it has previously been shown⁸ that the lower boundary of the gap is strongly affected by the presence of salts. This has recently been studied in more detail by measuring cloud point temperatures for 1% PEO solutions containing various alkali halides as functions of the salt concentrations.⁹ The alkali halides generally lowered the cloud point in different amounts—the only exception found was KI, which at low concentrations raised the cloud point slightly. The negative ion present dominated the clouding behavior of the system, the order of effectiveness being $\text{F}^- > \text{Cl}^- > \text{Br}^- > \text{I}^-$ (F^- lowered the cloud point the most). Among the alkali ions K^+ had the largest effect, but it was closely followed by the others in the following order: $\text{K}^+ \approx \text{Rb}^+ > \text{Na}^+ \approx \text{Cs}^+ > \text{Li}^+$. To rationalize these differences found in influence on clouding between the various alkali halides, a zone with decreased salt concentration was assumed to exist around the chains. The sizes of these zones were, for the different electrolytes, correlated to their abilities to lower the cloud point (cf. ref 9).

When NMR is now employed for further investigations on these three component systems, the aim is to gain more insight into their physical properties and to understand the mechanisms of the salt effects better. The number of NMR investigations of this kind is—as far as known—very sparse. Maijgren¹⁰ has measured ^{81}Br line widths of RbBr in the presence of very low concentrations (ppm) of high molecular weight PEO in aqueous solutions. Sugawara et al. studied the ^{35}Cl line width of KCl in an oligomeric (approximately tetrameric) PEO-water mixture.¹¹ Further, support for formation of a complex between Na^+ and PEO in acetonitrile has been found by Ricard.¹² Under certain circumstances, he found two ^{23}Na lines corresponding to bound and free sodium, respectively, in the system. In the present paper, the interest has been directed toward aqueous solutions of moderately high molecular weight PEO (the degree of polymerization ≈ 110) in a concentration interval up to 60% by weight. Alkali halides with nuclei that are suitable for NMR experiments have been added and the relaxation times for various salt nuclei have been measured as functions of the PEO concentration.

Experimental Section

The experiments were performed with PEO of three different molecular weights: most frequently a molecular weight of 4820 ($M_w/M_n = 1.04$ from Polymer Laboratories, Shrewsbury, U.K.) was used, but for some investigations molecular weights of 998 ($M_w/M_n = 1.06$ from the same source) and of 4×10^6 (Polyox WSR-301 from Union Carbide Corp.) were employed. In the following, when the molecular weight of PEO is not explicitly

mentioned, the medium-sized material is referred to. The polymers were dried for at least 24 h at 40 °C under vacuum. All salts were of Merck's suprapure quality except for KF , which was of pro analysi grade. They were dried at a temperature above 200 °C for a minimum of 24 h. Due to its hygroscopicity, LiCl was instead dried in a vacuum oven at 150 °C overnight. The water used was doubly distilled and saturated with deoxygenated nitrogen, in order to remove dissolved oxygen.

The samples containing the high molecular weight PEO were prepared according to the procedure described elsewhere.⁹ In the other cases, the substances were directly weighed into NMR tubes; the tubes were shaken and left overnight to equilibrate.

The NMR measurements were performed with a Bruker CXP-100 spectrometer operating at the following frequencies: ^7Li , 34.98 MHz; ^{23}Na , 23.81 MHz; ^{133}Cs , 11.81 MHz; ^{35}Cl , 8.82 MHz; and ^{81}Br , 24.31 MHz. For the determination of longitudinal relaxation times (T_1) the fast inversion-recovery technique was used and T_1 was calculated from nonlinear curve fittings to the intensities obtained for 18 different τ values in each case. The transverse relaxation times (T_2) were measured from the line widths after corrections for field inhomogeneities. The agreement between the two relaxation times was always very good. For ^{81}Br , only T_2 was measured for the polymer-containing samples. To avoid problems due to acoustic ringing, the compensation scheme recently proposed by Patt¹³ was applied to the broadest ^{35}Cl and ^{81}Br lines.

Values of T_1 were generally determined once per sample—several checks with repeated measurements on some of the samples indicated that the reproducibility was excellent. The line widths were usually taken from two to three spectra. The precision in the T_2 determinations was less than in that of T_1 .

Generally, the measurements were performed at 25.6 ± 0.3 °C (the temperature of the magnet). Otherwise, the temperature was set and controlled by B-VT 1000 variable-temperature equipment and it was estimated to be stable within ± 0.5 °C. At elevated temperatures, the samples were always contained in sealed glass tubes.

NMR Methods

All the nuclei studied have spin quantum numbers, I , of $3/2$ and accordingly they possess electric quadrupolar moments. Except for ^7Li , quadrupolar relaxation is the dominating relaxation mechanism.¹⁴ It is caused by the interaction between fluctuating field gradients—the time dependence of which stems from molecular motions of the surrounding solvent molecules—and nuclear quadrupole moments. Under extreme narrowing conditions, i.e., when the frequency of modulation of the quadrupolar interaction is rapid compared to the Larmor frequency of the nucleus, the relaxation of these nuclei is described by a single-exponential function. Then, the longitudinal and the transverse relaxation rates, $1/T_1$ and $1/T_2$, become equal and are, for the case with axially symmetric field gradients, given by¹⁵

$$\frac{1}{T_1^Q} = \frac{1}{T_2^Q} = \frac{3\pi^2}{10} \frac{2I+3}{I^2(2I-1)} \left(\frac{e^2 q_{zz} Q}{h} \right)^2 \tau_c \quad (1)$$

where all symbols have their usual meanings.

In the extreme narrowing case, which is valid for the measurements presented here, the relaxation rate is thus proportional to the product of the square of the electric field gradient (q_{zz}) and the correlation time (τ_c). Resolution of this product into its constituent factors is not possible without further pieces of information. For less complicated systems, several models for estimating the field gradient fluctuation and/or the correlation time separately have been presented. According, e.g., to Hertz's electrostatic theory,^{16,17} the field gradients are created by a distribution of point charges surrounding the nucleus. These field gradients undergo thermal fluctuations and cause thereby relaxation. The distortions from spherical symmetry of

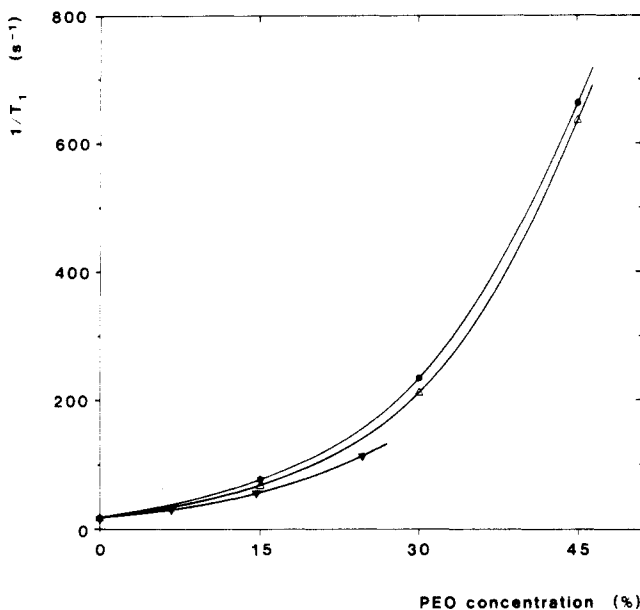


Figure 1. Relaxation rates at 25.6 °C of ^{23}Na in aqueous solutions of NaF (0.4 *m*, ∇), NaCl and NaBr (1.0 *m*, Δ ; the results for the two salts very nearly coincide), and NaI (1.0 *m*, \bullet) as a function of the concentration of PEO (given as the weight ratio of PEO to PEO and water, expressed in percentage).

the closed electron shells are considered by using Sternheimer antishielding factors. Hynes and Wolynes¹⁸ have formulated an electrostatic continuum theory for the quadrupolar relaxation rate and recently Engström, Jönsson, and Jönsson¹⁹ have published a purely molecular approach to the problem employing the Monte Carlo simulation technique to calculate fluctuations of electric field gradients. All these estimations have been developed for pure aqueous electrolyte solutions of—generally—low concentrations. The system investigated in this paper is more complex; therefore, a similar treatment is not possible at the present time.

For ^7Li , both quadrupolar and magnetic dipole-dipole relaxation contribute to the total relaxation rate measured. In order to separate the contributions from the two mechanisms, the intermolecular nuclear Overhauser enhancement (NOE) was measured. Therefrom the ^1H - ^7Li part of the dipole-dipole relaxation rate could be established.

The NOE factor (η) is obtained from the ratio between the intensities of the ^7Li signals with (I_{ir}) and without (I_0) irradiation at the proton frequency:¹⁵

$$I_{\text{ir}}/I_0 = 1 + \eta \quad (2)$$

The ^1H - ^7Li dipolar contribution to the relaxation rate, $(T_1^{\text{D}})^{-1}$, is given by²⁰

$$\frac{1}{T_1^{\text{D}}} = \eta \frac{2\gamma_{^7\text{Li}}}{\gamma_{^1\text{H}}} \frac{1}{T_1} \quad (3)$$

where γ is the magnetogyric ratio of the nucleus. The remaining relaxation rate can be calculated as the difference between the total relaxation rate and $(T_1^{\text{D}})^{-1}$. This contribution should mainly be due to quadrupolar and ^7Li - ^7Li dipolar relaxation. In pure aqueous LiCl solutions the latter contribution is known to be negligible up to a concentration of 5–6 *m* and to be of minor importance over the remaining concentration interval.²¹ It is thus probably negligible for the solutions studied here too; therefore, the quadrupolar relaxation rate, $(T_1^{\text{Q}})^{-1}$, is assumed to be

$$1/T_1^{\text{Q}} = 1/T_1 - 1/T_1^{\text{D}} \quad (4)$$

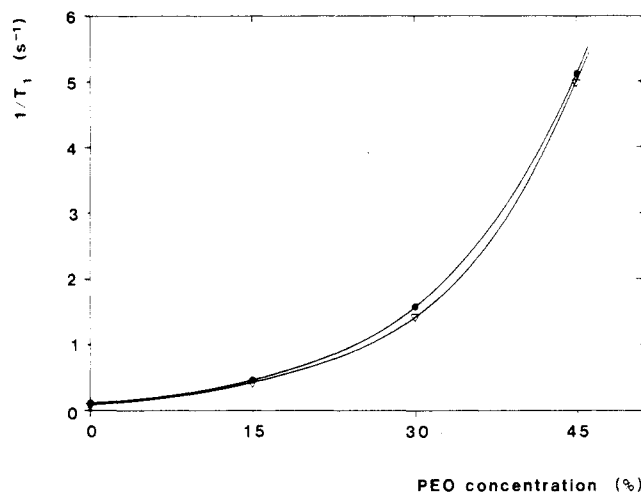


Figure 2. Relaxation rates at 25.6 °C of ^{133}Cs in 1.0 *m* aqueous solutions of CsCl (∇) and CsBr (\bullet) as a function of the concentration of PEO.

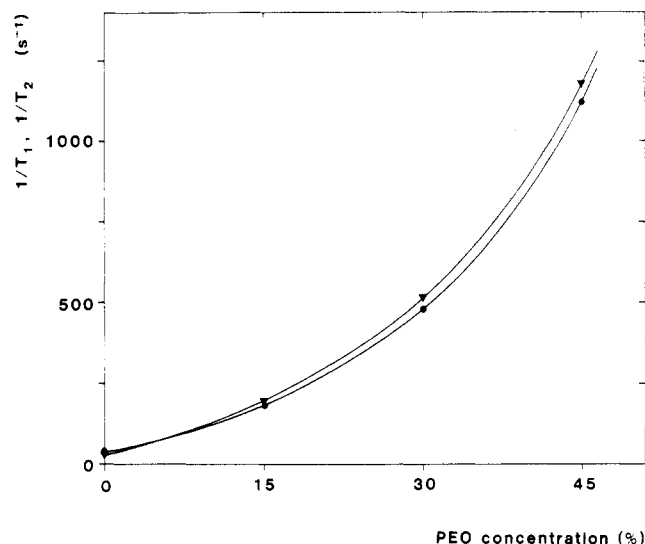


Figure 3. Relaxation rates at 25.6 °C of ^{35}Cl in 1.0 *m* aqueous solutions of NaCl (∇) and CsCl (\bullet) as a function of the concentration of PEO.

Results and Discussion

Measurements at the Magnet Temperature. Relaxation rates of various alkali and halide nuclei have been determined as functions of the polymer concentration in PEO-water-alkali halide solutions. In Figures 1–4 the relaxation rates for ^{23}Na , ^{133}Cs , ^{35}Cl , and ^{81}Br , respectively, are plotted. The salt concentration was 1.0 *m* except in the case of NaF, where it had to be reduced to 0.4 *m* due to the low solubility of the salt. (Pure aqueous solutions with up to 1.0 *m* of NaF can be prepared,²² but addition of PEO reduces the solubility.) Generally, both the spin-lattice and the spin-spin relaxation times (T_1 and T_2) have been determined and the mutual agreement between them is very good. Since T_1 could be established with higher precision, it has been used in the figures, when there is a choice. A further increase of the PEO concentration up to 60% does—at least for NaBr—not seem to change the patterns shown in Figures 1–4. A 1.0 *m* NaBr solution with 60% PEO has a T_1 for ^{23}Na of 0.614 ms, which—if compared to Figure 1—agrees well with an extrapolation of the curve for lower PEO contents.

Measurements of T_1 and η (the NOE factor) for ^7Li in LiCl-PEO- H_2O mixtures have been performed for different PEO contents and the contributions from the two

Table I
Relaxation Rates of ^7Li in Samples Containing 1.0 *m* LiCl and Variable Amounts of PEO^a

[PEO], %	T_1 , s	$10^2(1/T_1)$, s ⁻¹	η	fraction due to dipole-dipole relaxn, %	T_1^Q , s	$10^2(1/T_1^Q)$, s ⁻¹	T_1^D , s	$10^2(1/T_1^D)$, s ⁻¹
0	19.21	5.21	0.748	58.1	45.88	2.18	33.04	3.03
15.0	10.55	9.48	0.591	45.9	19.52	5.12	22.97	4.35
30.0	4.79	20.88	0.412	32.0	7.05	14.18	14.96	6.68
45.0	1.96	51.07	0.328	25.5	2.63	38.02	7.68	13.02

^a For details, see text.

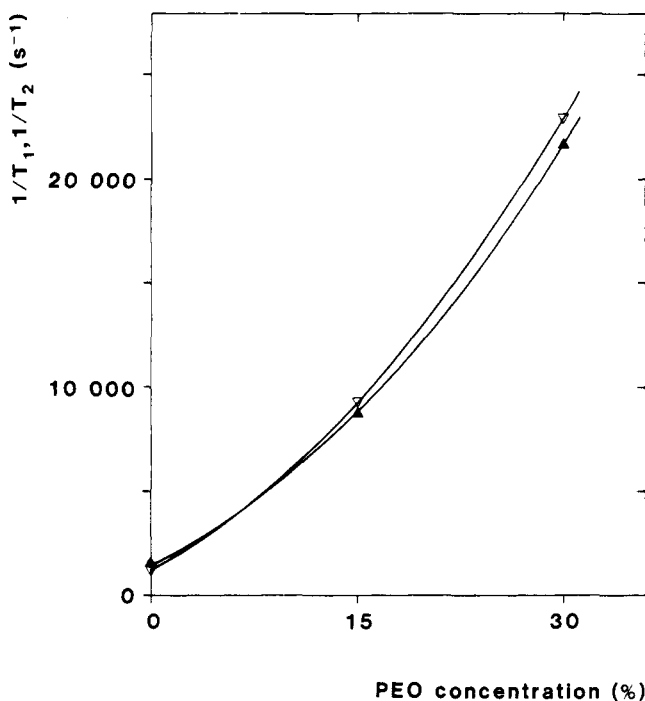


Figure 4. Relaxation rates at 25.6 °C of ^{81}Br in 1.0 *m* aqueous solutions of NaBr (∇) and CsBr (Δ) as a function of the concentration of PEO.

mechanisms discussed have been calculated from eq 3 and 4 (see Table I). The effect of adding PEO is substantially greater on the quadrupolar than on the dipolar relaxation rate, but both relaxation rates increase. In the following, when comparisons are made with the other alkali and halide nuclei, only the quadrupolar part of the ^7Li relaxation rate is considered.

In Figures 5 and 6 the relaxation rates of ^{23}Na and ^{35}Cl in samples containing PEO of different molecular weights have been compared. (For the high molecular weight PEO the viscosity of the solutions containing more than 4–5% PEO became so high that the practical handling of the samples was severely aggravated. For the low molecular weight polymers no such problems occurred.) The relaxation rates are shown to fall on the same curves irrespectively of the molecular weight of PEO. In fact, for those polymer concentrations where several molecular weights of PEO have been compared directly, the variations of T_1 are less than 5% with no signs of any systematic deviations. Thus, no dependence on the degree of polymerization—over the interval investigated—has been found.

The general feature of the results presented in Figures 1–4 and Table I is that addition of PEO affects the relaxation rates of both the halide and the alkali metal nuclei to a very large extent. This is markedly different from the relaxation of methylene protons of PEO in water, which is not at all affected when salt is added,²³ not even if it is added up to the cloud point concentration at the tem-

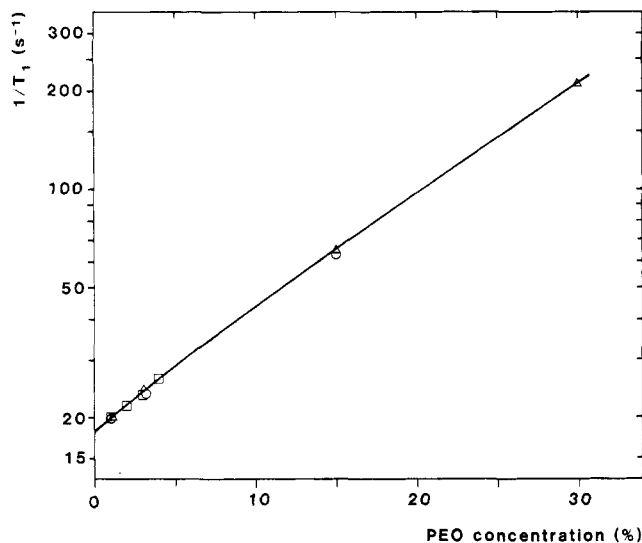


Figure 5. Comparison of the relaxation rates of ^{23}Na at 25.6 °C in aqueous solutions containing 1.0 *m* NaCl and PEO of different molecular weights (\square : 4×10^6 ; Δ : 4820; and \circ : 998).

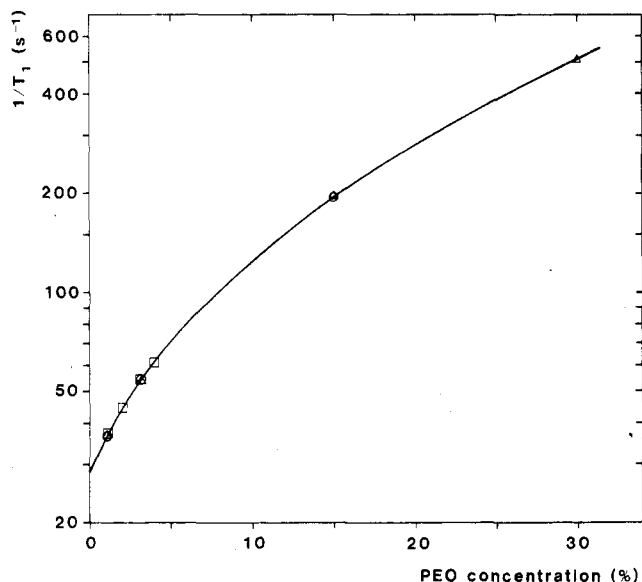


Figure 6. Comparison of the relaxation rates of ^{35}Cl at 25.6 °C in aqueous solutions containing 1.0 *m* NaCl and PEO of different molecular weights (\square : 4×10^6 ; Δ : 4820; and \circ : 998).

perature in question. To compare the effects on the different salt nuclei, the variation of the nuclear constants in eq 1 has to be eliminated. Therefore, the ratios of the relaxation rates for a certain nucleus in solutions with and without PEO—but with the same salt molality—have been calculated. These ratios have been depicted as functions of the PEO concentrations in Figure 7 for the alkali metal nuclei and in Figure 8 for the halide nuclei. There, the substantial increases in relaxation rates are obvious. For the alkali metals, the influence of the counterions seems

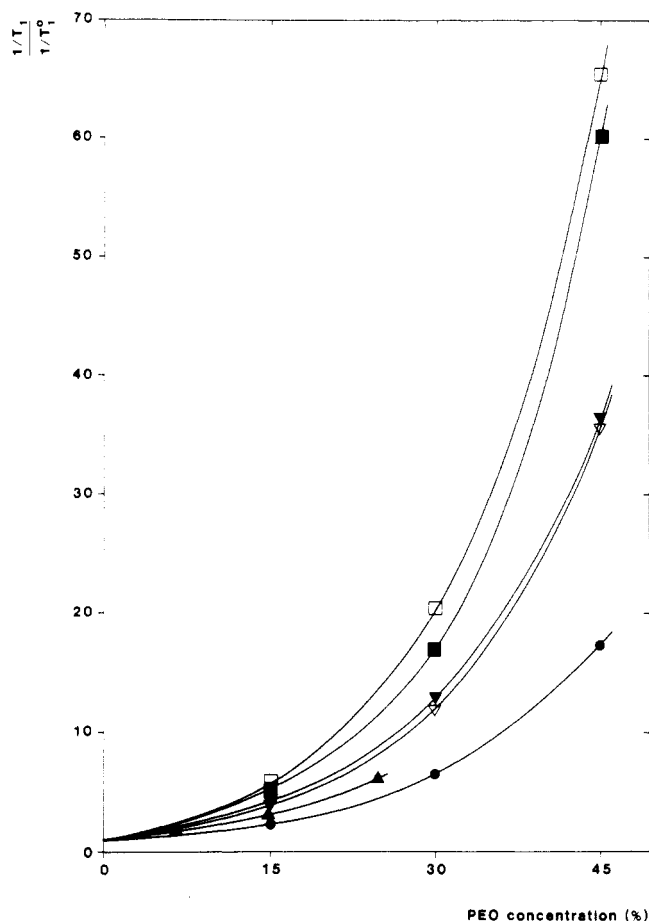


Figure 7. Increase in relaxation rate of alkali metal nuclei due to addition of PEO, expressed as $(1/T_1)/(1/T_1^0)$, where the superscript zero refers to the pure aqueous electrolyte solution with the same salt concentration (i.e., 1.0 *m* except for NaF). For the different nuclei, the following notations are used: ^7Li , circles (note that only the quadrupolar part of the ^7Li relaxation is used in this comparison; for details see text); ^{23}Na , triangles; and ^{133}Cs , squares. The symbols employed for the various salts are the following: LiCl , \bullet ; NaF , \blacktriangle (note that the salt concentration is 0.4 *m* in this case); NaCl and NaBr , ∇ (the results for the two salts very nearly coincide, the values for NaBr being always slightly larger than those for NaCl); NaI , \blacktriangledown ; CsCl , \blacksquare ; and CsBr , \square .

to be limited, which is demonstrated in Figure 7, where the curves for ^{133}Cs , ^{23}Na , and ^7Li fall in categories according to the kind of cation but irrespectively of the anion present. Note that the curve for NaF is measured at a salt concentration of 0.4 *m*, when all the others are valid for 1.0 *m* of salt. It was checked, though, that all the ^{23}Na curves for the lower salt concentration are close to the NaF curve shown, the order of the anion effects being I^- , Br^- , Cl^- , and F^- , where I^- has the largest influence. The relative relaxation rates of the halide nuclei in Figure 8, on the other hand, are clearly affected by the nature of the counterion present. No classification of the curves according to the observed nuclei, as in Figure 7, could be made in this case.

In the paper on salt effects on the cloud point,⁹ it was shown that the PEO chains most likely are surrounded by zones with a decreased salt concentration. Of course, such zones diminish the amount of water available for the ions; therefore, the salt concentration in the bulk phase is higher than the gross one, based on the total composition of the sample. Since the majority of the ions reside in the bulk solution—at least for low and moderate PEO contents—this increase in salt concentration should be reflected in the relaxation rates. From measurements on pure aqueous solutions of alkali halides, it is well-known that the re-

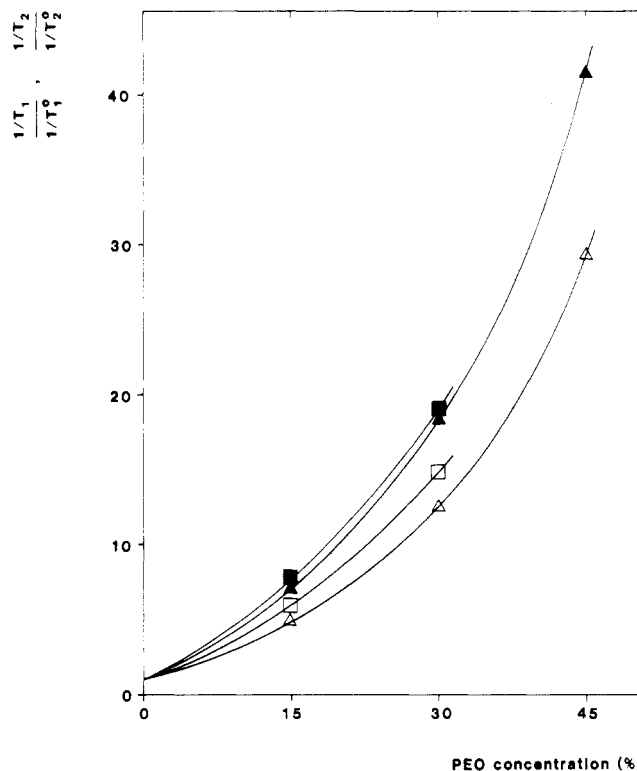


Figure 8. Increase in relaxation rate of halide nuclei due to addition of PEO, expressed as $(1/T_1)/(1/T_1^0)$ or $(1/T_2)/(1/T_2^0)$. The superscript zero refers to the pure aqueous electrolyte with the same salt concentration (i.e., 1.0 *m*). For the different nuclei, the following notations are used: ^{35}Cl , triangles; ^{81}Br , squares. The symbols employed for the various salts are the following: NaCl , \blacktriangle ; CsCl , \triangle ; NaBr , \blacksquare ; and CsBr , \square .

laxation rates are raised for the nuclei studied, when their concentrations are increased.²⁴⁻²⁶ Generally, this increase is less than a factor 5 even for very high salt concentrations (i.e., over 10 *m*) and in the low concentration range (i.e., up to 1 *m*) the effect is approximately negligible. For low and medium PEO contents the increment in salt concentration of the bulk solution should be quite limited. Hence, this effect cannot be the reason for the large increases of the relaxation rates.

The next issue to consider is the influence of asymmetric hydration. By the concept of asymmetric hydration it is meant that the arrangement of solvent water molecules around an ion is distorted by the presence of other species in the solution. The more symmetric the hydration of a quadrupolar nucleus, the lower is its relaxation rate (which is, e.g., demonstrated for salts at finite concentrations compared to those at infinite dilution²⁴⁻²⁶). PEO is known to affect the water molecules in its immediate proximity and it is also probable that this influence may range over several layers of water.²⁷ Ions that penetrate more or less into this zone of structured water will be affected, since their surrounding water shells should be disturbed, and accordingly the relaxation times should be shorter than in pure water. To estimate the magnitudes of these effects, comparisons can be made with other systems. The influence of the degree of polymerization of PEO on the relaxation rates of alkali metal and halide nuclei has been shown to be negligible (Figures 5 and 6). The influences of changes in translational diffusion—which should be increasingly slower the higher the molecular weight of PEO—therefore seems to be of minor importance; consequently, a comparison with model solutions containing smaller molecules is justified. Such systems are, for instance, salt–water solutions with methanol or ethanol (see,

e.g., ref 28 and 10), acetone,²⁹ dimethyl sulfoxide,³⁰ or a simple amide³¹ as the third component. Any of these additives influences the relaxation rates of the ionic nuclei substantially. Typically a maximum increase by a factor of around 10–12 is found for the halide nuclei, while the alkali metal nuclei are affected less (not more than 5–7 times), when in most cases the whole solvent composition interval has been investigated. Asymmetric hydration of the ions, caused by the presence of the organic solutes, is assumed to explain the large increases in relaxation rate. This mechanism is certainly of importance in the PEO system as well.

For aqueous solutions of tetraalkylammonium compounds relaxation rates for the halide nuclei that are approximately 5–10 times larger than those at infinite dilution can be found already for salt concentrations below 1 *m*.^{10,32–24} For concentrated solutions, such effects are even greater (e.g., a factor of 40–50 for 6.8 *m* of tetraethylammonium bromide³²). These salts are known to form solid clathrate hydrates³⁵ and their extreme effects on the relaxation are supposed to be due to the increased water structure formation around the cations. The comparison with the PEO case is not as straightforward as with the alcohols and similar substances mentioned above, since the concentration of the tetraalkylammonium ions and that of the nucleus followed by NMR cannot be varied independently. Anyhow, asymmetric hydration is believed mainly to account for the changes in relaxation rate, and it is demonstrated that such changes can be large for halide ions under these circumstances.

Thus, increased salt concentration and asymmetric hydration are factors that certainly affect the relaxation rates in PEO-containing systems. Analogies with the tetraalkylammonium compounds add the information that such effects can be large enough to explain the halide nuclei measurements here presented. However, it is clearly indicated in the literature that the effects on the alkali ions generally are substantially smaller, which is contradictory to the results for the PEO systems. Obviously, a further mechanism that could be responsible for the rapid relaxation of the alkali metal nuclei in PEO-containing mixtures should be searched for.

In metal ion complexes with crown ethers and similar compounds the positive ions are known to interact directly with the ether oxygens.^{36,37} These complexes can be very stable in organic solvents but are generally substantially weaker in water, due to the competition with the favorable hydration of the ions in the latter case.^{38,39} Furthermore, direct ion–ether oxygen interactions have also been observed for some much weaker complexes between various acyclic polyethers and alkali metal ions in organic solvents.^{12,40,41} The ligands are there supposed to wrap themselves in a helical manner around the metal ion—a conformation which is similar to that found for the solid states (when existing) of these complexes.

If any “complexes” similar to the crown ether ones exist in aqueous PEO solutions, they are likely to be weak, both because of the properties of the solvent and also since no stable polyether rings with a suitable geometry for the ions exist permanently. However, if the oxygen contacts have very large effects on the relaxation—which is most likely, judging from the crown ether measurements⁴²—only very few of the ions have on an average to be involved for the increase in relaxation rate to become substantial. It thus seems very reasonable that direct ion–ether oxygen contacts do contribute to the relaxation of alkali metal nuclei in aqueous PEO solutions. Thereby the differences found, as compared to other aqueous salt solutions containing

Table II
Activation Energies for the Relaxation Rates Obtained from Linear Least-Squares Fits in the Temperature Intervals Indicated for Aqueous Salt Solutions (1.0 *m*) Generally Containing PEO

salt	nucleus	[PEO], %	temp interval, °C		activation energy, kJ/mol
			lower limit	upper limit	
NaBr	⁸¹ Br	0	25	90	11.8
		15.00	25	110	21.6
NaCl	²³ Na	15.00	–10	25	34.7
		29.99	–10	25	41.5
		45.00	–5	25	41.7
NaBr	²³ Na	0	8	90	10.7
		15.00	15	55	25.8
		30.02	15	55	32.9
		44.96	15	55	38.8

organic solutes (alcohol, etc.) discussed above, can be understood.

There remains to remark on the effect or lack of effect of counterions in Figures 7 and 8. The alkali metal ions—which are followed spectroscopically in Figure 7—are in general smaller, less polarizable, and more strongly hydrated than the halide ions. They should therefore not be very sensitive to the presence of the various halide ions. Besides, the cation–ether oxygen interactions, which increase the relaxation rates of the alkali metal nuclei substantially, may be of varying strengths depending on the kind of cation. Both circumstances mentioned should favor a pattern like that in Figure 7, where the counterion effects are fairly limited. In Figure 8 the situation is reversed. There the halide nuclei are followed by NMR and, apparently, the counterions have a greater influence than in Figure 7. This is not unique for the PEO-containing system, but is also found, e.g., in pure aqueous alkali halide solutions.^{25,26} The relaxation of the halide nuclei is affected by species that disturb the time-dependent arrangement of solvent molecules around them. Here, both PEO and the alkali metal ions are strongly hydrated and, thereby, are possible sources of disturbances. As discussed above, the increased water structure formation around PEO is probably the major reason for the large effects of asymmetric hydration (and for the large increases in relaxation rates) sensed by the halide nuclei. If this water structure is affected more efficiently by the cation with the strongest hydration shell (i.e., Na⁺ in this case), it is reasonable that that ion should also induce a more pronounced counterion effect upon the relaxation of the halide nuclei. This is in accord with the results in Figure 8, where Na⁺ has a larger influence than Cs⁺, which indicates that the most strongly hydrated and less polarizable of the two cations investigated has the largest effect.

To conclude, it seems reasonable that the large effects of addition of PEO to aqueous alkali halide solutions on the relaxation rate of alkali metal and halide nuclei are due to a combination of different effects: (1) increase in salt concentration of the bulk solution due to hydration of polymer chains (gives only a minor contribution), (2) asymmetric hydration of the ions as a consequence of the PEO–water interaction, and (3) direct interaction between the positive ions and ether oxygens of the polymer.

Measurements at Different Temperatures. The variation of the relaxation rate with temperature has been investigated for two nuclei, ²³Na and ⁸¹Br. For bromine (see Figure 9), a linear relation between log (1/*T*₂) and 1/*T* was found both for a pure aqueous NaBr solution and for a similar sample containing PEO at temperatures between 25 and 110 °C. From the Arrhenius equation 1/*T*_{1,2} ∝ $e^{E/RT}$, activation energies have been calculated (Table II)

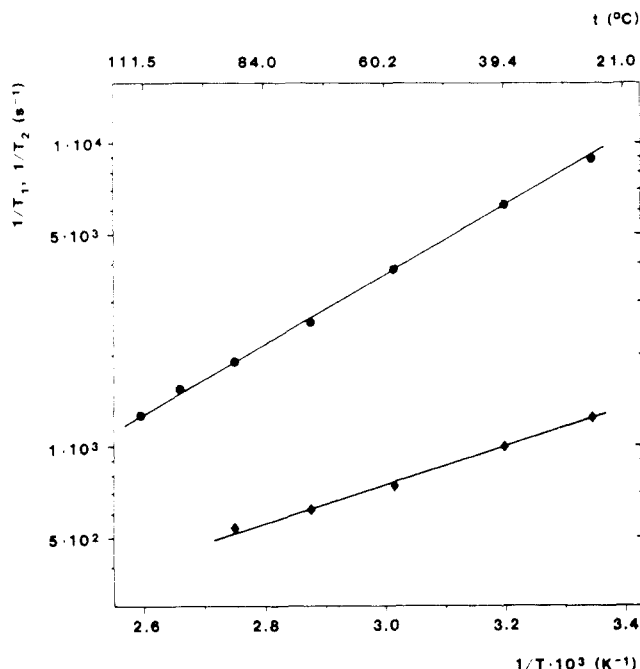


Figure 9. Logarithm of the relaxation rate of ^{81}Br as a function of $1/T$ for a pure aqueous solution of 1.0 *m* NaBr (◆) and for the same solution containing 15% PEO (●).

for the two samples studied. The value obtained for the pure NaBr–H₂O case agrees reasonably well with literature data (10.6 kJ/mol for 1 *m* NaBr⁴³) while the presence of PEO substantially raises the activation energy. Since the relaxation rate of a quadrupolar nucleus is highly dependent on the arrangement of the solvent molecules surrounding it, the pure salt–water value of the activation energy is related to the mobility of the solvent water molecules in that case. PEO tends to stabilize the water structure;²⁷ therefore, it is reasonable that this should be manifested in a larger activation energy. This is also found for the ^{81}Br relaxation in 15% PEO (see Table II).

The temperature dependence for the ^{23}Na relaxation rate shows a similar behavior for NaCl-containing PEO–water samples observed from room temperature toward the freezing point ($\sim -15^\circ\text{C}$). The activation energies obtained (see Table II) are 3–4 times larger than the value for NaCl in liquid water (the literature value for the latter is 12.1 kJ/mol in 3.0 M NaCl,⁴³ while it is 10.4 kJ/mol in 1 *m* NaBr⁴⁴). When the ^{23}Na relaxation is followed over a larger temperature interval (0–110 $^\circ\text{C}$ and NaBr-containing samples), it is clear that the linear relation between $\log(1/T_1)$ and $1/T$ no longer holds (see Figure 10). That addition of PEO raises the activation energy in this case also can be seen in Table II. A linear least-squares fit has been made to the three upper curves in Figure 10 for 15–55 $^\circ\text{C}$ and the activation energies have been calculated therefrom. As for ^{81}Br , the activation energy is substantially larger the higher the PEO concentration. This could be explained in the same way for ^{23}Na as for ^{81}Br above.

To rationalize the curvatures found in the ^{23}Na data, it is necessary to consider the mechanisms that are involved in the relaxation. If several processes with different temperature dependences contribute, the results would probably show nonlinear behaviors. Apart from the important cation–ether oxygen contacts, the relaxation processes are essentially the same for all nuclei studied. Since the temperature-dependent data for ^{23}Na indicate that other processes than those for ^{81}Br should contribute, this is further support for the necessity to include the ion–ether

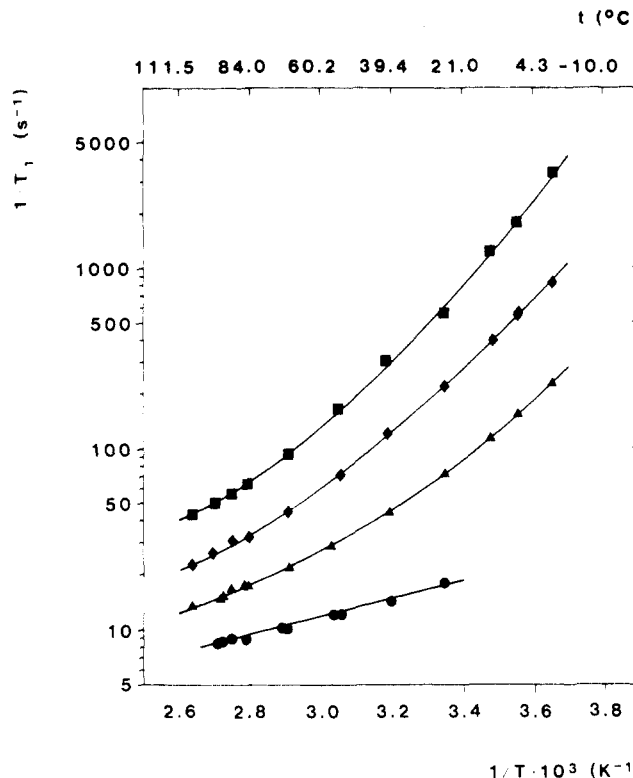


Figure 10. Logarithm of the relaxation rate of ^{23}Na as a function of $1/T$ for aqueous NaBr solutions (1.0 *m*) containing various amounts of PEO: 0%, ●; 15%, ▲; 30%, ◆; and 45%, ■.

oxygen mechanism for the relaxation of positive ions in aqueous PEO solutions.

Additional support for this can be obtained from Figure 11, where the ^{81}Br and ^{23}Na relaxation rates at temperatures below but close to the cloud point (which appears at ~ 120 – 125°C) are shown. Apparently, the ^{81}Br relaxation rate approaches that of the pure aqueous NaBr (extrapolated to the higher temperatures) while that of ^{23}Na only levels off. The salt-deficient zones shrink and the increased structure of water around PEO is weakened at higher temperatures.⁹ The polymer chains—which at room temperature have fairly extended conformations—should contract when the temperature is raised, to obtain their unperturbed dimensions at the Θ -temperature (in this case around 90°C). The contraction should continue further at even higher temperatures and above the cloud point the system phase separates. It is reasonable that the ions are expelled from the neighborhoods of the chains to the bulk solution, when the polymer becomes tightly coiled. The majority of the ions should therefore be in a water milieu which becomes less affected by the presence of PEO the higher the temperature. For the nuclei studied, a PEO–water solution should thus from an NMR point of view become more similar to a pure aqueous electrolyte solution at elevated temperatures. The approach of the ^{81}Br curve for the PEO-containing sample in Figure 11 nearer to that for the pure aqueous one probably reflects a mechanism of this kind. For ^{23}Na the situation is different, since the relaxation of this nucleus includes contributions additional to those mentioned for ^{81}Br (i.e., cation–ether oxygen interactions). The contacts between the Na^+ ions and the ether oxygens of PEO should be facilitated when the salt-deficient zones shrink. Furthermore, those Na^+ ions that actually appear close to PEO when the chains become tightly coiled at elevated temperatures may have better possibilities to interact effectively with the ether oxygens and thereby to give larger

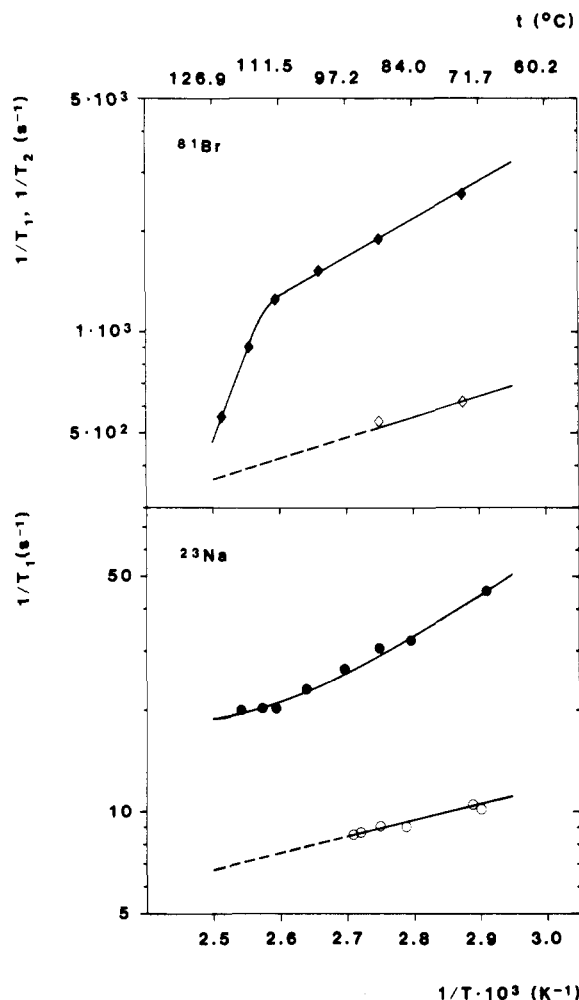


Figure 11. Details of the relaxation rates of ^{81}Br and ^{23}Na vs. $1/T$ at high temperatures. Nucleus: ^{81}Br , squares, and ^{23}Na , circles. The open symbols denote the pure aqueous 1.0 m NaBr sample, while the filled ones should be interpreted as follows: \blacklozenge , 1.0 m NaBr, 15% PEO; and \bullet , 1.0 m NaBr, 30% PEO.

contributions to the relaxation rate than those in PEO solutions at lower temperatures. Thus, in the ^{23}Na case, a balance may exist at elevated temperatures between effects that tend to lower and to raise the relaxation rate. The expulsion of the ions out into the bulk water solutions—which was the only mechanism discussed for ^{81}Br —tends to lower the relaxation rate, while the increased ion-ether oxygen interactions can raise it. Apparently the latter effect dominates, since the ^{23}Na curve in Figure 11 levels off at high enough temperatures. This lends further support to the existence of interactions between alkali metal ions and ether oxygens in PEO-water-salt systems.

Relevance in Relation to Thermodynamic Data

When one compares the thermodynamic cloud point measurements⁹ with the magnetic relaxation investigations presented here, it is obvious that different pieces of information can be extracted from the two types of experiments. The salt effects on the cloud point primarily reflect the extensions of the salt-deficient zones surrounding the chains. These zones are formed mainly as a consequence of an image charge force effect and result, e.g., in an increased bulk salt concentration. The slightly larger salt concentration gives only a minor contribution to the relaxation rates measured. On the other hand, asymmetric hydration accounts for an important part of the relaxation rates (for the halide nuclei certainly the major part), which

it can only do if the stabilizing effects of PEO upon the water structure are at least fairly extensive. Thus, indirect support for the increased structuring is obtained. Finally, the cation-ether oxygen interactions that are only apparent in the NMR results most likely only involve a very small proportion of the cations. Therefore, they do not exhibit thermodynamic consequences.

To conclude, it is obvious that some, but limited, support for the molecular view of the system that was a basis in the thermodynamic paper⁹ has been gained from the present NMR measurements. None of the results in this work is incompatible with the previous model, but apparently experiments of other types are needed to further elucidate the proposed ideas.

Acknowledgment. I thank Jan Christer Eriksson, Ulf Henriksson, and Roland Kjellander for fruitful discussions in connection with this work. With the practical handling of the NMR apparatus Ulf Henriksson and Tomas Klason have been most helpful. This work has received financial support from the Swedish Natural Science Research Council and from Bengt Lundqvist Memorial Foundation.

Registry No. PEO (SRU), 25322-68-3; NaF, 7681-49-4; NaCl, 7647-14-5; NaBr, 7647-15-6; NaI, 7681-82-5; CsCl, 7647-17-8; CsBr, 7787-69-1; LiCl, 7447-41-8.

References and Notes

- (1) Liu, K.-J.; Anderson, J. E. *Macromolecules* **1970**, *3*, 163.
- (2) Liu, K.-J.; Ullman, R. *J. Chem. Phys.* **1968**, *48*, 1158.
- (3) Brown, W.; Stilbs, P. *Polymer* **1982**, *23*, 1780.
- (4) Liu, K.-J.; Parsons, J. L. *Macromolecules* **1969**, *2*, 529.
- (5) Connor, T. M.; McLauchlan, K. A. *J. Phys. Chem.* **1965**, *69*, 1888.
- (6) Lang, M.-C.; Lauprêtre, F.; Noël, C.; Monnerie, L. *J. Chem. Soc., Faraday Trans. 2* **1979**, *75*, 349.
- (7) Saeki, S.; Kuwahara, N.; Nakata, M.; Kaneko, M. *Polymer* **1976**, *17*, 685.
- (8) Bailey, F. E., Jr.; Callard, R. W. *J. Appl. Polym. Sci.* **1959**, *1*, 56.
- (9) Florin, E.; Kjellander, R.; Eriksson, J. C. *J. Chem. Soc., Faraday Trans. 1* **1984**, *80*, 2889.
- (10) Majgren, B. Thesis, The Royal Institute of Technology, Stockholm, Sweden, 1974.
- (11) Sugawara, T.; Yudasaka, M.; Yokoyama, Y.; Fujiyama, T.; Iwamura, H. *J. Phys. Chem.* **1982**, *86*, 2705.
- (12) Ricard, A. *Eur. Polym. J.* **1979**, *15*, 1.
- (13) Patt, S. L. *J. Magn. Reson.* **1982**, *49*, 161.
- (14) Lindman, B.; Forsén, S. In "NMR and the Periodic Table"; Harris, R. K., Mann, B. E., Eds.; Academic Press: London, 1978; Chapters 6C and 13A.
- (15) Harris, R. K. In "NMR and the Periodic Table"; Harris, R. K., Mann, B. E., Eds.; Academic Press: London, 1978; Chapter 1.
- (16) Hertz, H. G. *Ber. Bunsenges. Phys. Chem.* **1973**, *77*, 531.
- (17) Hertz, H. G. *Ber. Bunsenges. Phys. Chem.* **1973**, *77*, 688.
- (18) Hynes, J. T.; Wolynes, P. G. *J. Chem. Phys.* **1981**, *75*, 395.
- (19) Engström, S.; Jönsson, B.; Jönsson, B. *J. Magn. Reson.* **1982**, *50*, 1.
- (20) Webb, G. A. In "NMR and the Periodic Table"; Harris, R. K., Mann, B. E., Eds.; Academic Press: London, 1978; p 80.
- (21) Hertz, H. G.; Tutsch, R.; Versmold, H. *Ber. Bunsenges. Phys. Chem.* **1971**, *75*, 1177.
- (22) Weast, R. C., Ed. "CRC Handbook of Chemistry and Physics"; CRC Press: West Palm Beach, FL, 1978; p B-160.
- (23) Liu, K.-J.; Anderson, J. E. *Macromolecules* **1969**, *2*, 235.
- (24) Hertz, H. G.; Holz, M.; Keller, G.; Versmold, H.; Yoon, C. *Ber. Bunsenges. Phys. Chem.* **1974**, *78*, 493.
- (25) Holz, M.; Weingärtner, H. *J. Magn. Reson.* **1977**, *27*, 153.
- (26) Hertz, H. G.; Holz, M.; Klute, R.; Stalidis, G.; Versmold, H. *Ber. Bunsenges. Phys. Chem.* **1974**, *78*, 24.
- (27) Kjellander, R.; Florin, E. *J. Chem. Soc., Faraday Trans. 1* **1981**, *77*, 2053.
- (28) Holz, M.; Weingärtner, H.; Hertz, H. G. *J. Chem. Soc., Faraday Trans. 1* **1977**, *73*, 71.
- (29) Yudasaka, M.; Sugawara, T.; Iwamura, H.; Fujiyama, T. *Bull. Chem. Soc. Jpn.* **1981**, *54*, 1933.
- (30) Yudasaka, M.; Sugawara, T.; Iwamura, H.; Fujiyama, T. *Bull. Chem. Soc. Jpn.* **1982**, *55*, 311.
- (31) Holz, M.; Rau, C. K. *J. Chem. Soc., Faraday Trans. 1* **1982**, *78*, 1899.

- (32) Lindman, B.; Forsén, S.; Forslind, E. *J. Phys. Chem.* **1968**, *72*, 2805.
 (33) Wennerström, H.; Lindman, B.; Forsén, S. *J. Phys. Chem.* **1971**, *75*, 2936.
 (34) Hertz, H. G.; Holz, M. *J. Phys. Chem.* **1974**, *78*, 1002.
 (35) Feil, D.; Jeffrey, G. A. *J. Chem. Phys.* **1961**, *35*, 1863.
 (36) Pedersen, C. J. *J. Am. Chem. Soc.* **1967**, *89*, 7017.
 (37) Truter, M. R. *Struct. Bonding (Berlin)* **1973**, *16*, 71.
 (38) Izatt, R. M.; Eatough, D. J.; Christensen, J. J. *Struct. Bonding (Berlin)* **1973**, *16*, 161.
 (39) Lin, J. D.; Popov, A. I. *J. Am. Chem. Soc.* **1981**, *103*, 3773.
 (40) Grandjean, J.; Laszlo, P.; Offerman, W.; Rinaldi, P. *J. Am. Chem. Soc.* **1981**, *103*, 1380.
 (41) Vögtle, F.; Weber, E. *Angew. Chem., Int. Ed. Engl.* **1979**, *18*, 753.
 (42) Shchori, E.; Jagur-Grodzinski, J.; Luz, Z.; Shporer, M. *J. Am. Chem. Soc.* **1971**, *93*, 7133.
 (43) Eisenstadt, M.; Friedman, H. L. *J. Chem. Phys.* **1966**, *44*, 1407.
 (44) Hall, C.; Richards, R. E.; Schulz, G. N.; Sharp, R. R. *Mol. Phys.* **1969**, *16*, 529.

Molecular Mechanism of the Ring-Flip Process in Polycarbonate

Jacob Schaefer* and E. O. Stejskal

Physical Sciences Center, Monsanto Company, St. Louis, Missouri 63167

Dennis Perchak,[†] Jeffrey Skolnick,[‡] and Robert Yaris

Department of Chemistry, Washington University, St. Louis, Missouri 63130

ABSTRACT: Calculations of the conformational preferences of isolated single chains of poly(2,6-dimethylphenylene oxide) (PPO) and bisphenol-A polycarbonate (PC) predict that the rings of both chains are nearly free rotors at room temperature. However, experimental dipolar rotational spin-echo ¹³C NMR shows that in the glass, the rings of PPO execute only small-amplitude motions while those of PC undergo primarily 180° ring flips (a hindered rotation) superimposed on some wiggles. Geometrical considerations of the dense packing of chains in the glass suggest that the rings of adjacent chains block rotational freedom. We propose that the mobility of the PC main chain results in lattice distortions which allow ring flips not permitted by the stiffer PPO main chain.

Introduction

Polycarbonates undergo a variety of large-amplitude molecular motions, some of which have been characterized recently by the collapse of deuterium quadrupolar,¹ carbon chemical shift,² and dipolar³ tensors. The dominant motion for bisphenol-A polycarbonate (PC) is 180° flips about the aromatic-ring C₂ symmetry axis. These flips occur over a broad range of frequencies centered about 300 kHz at room temperature. The flips are superimposed on 30° ring oscillations about the same axis. Other main-chain motions are also significant; amplitudes of these wiggling motions are of the order of 20° (root mean square).³

In this paper we demonstrate experimentally that poly(2,6-dimethylphenylene oxide) (PPO) and its methyl-brominated analogue have no large-amplitude motions in the glass at room temperature. We then relate the differences between microscopic molecular motions in PC and PPO to the differences in their anelastic mechanical loss behavior. This connection aids in the identification of a mechanically active lattice distortion in PC which we claim is ultimately responsible for its ring flips.

Experiments

Carbon dipolar tensors were characterized by using dipolar rotational spin-echo ¹³C NMR at 15.1 MHz with magic-angle spinning,⁴ usually at 1894 Hz. This is a two-dimensional experiment in which, during the additional time dimension, carbon magnetization is allowed to evolve under the influence of C-H coupling while H-H coupling is suppressed by homonuclear multiple-pulse (WAHUA) decoupling.^{5,6} For singly protonated carbons whose resonances are well resolved in the chemical shift dimension, a Fourier transform of the intensity at the peak maximum vs. evolution time yields a dipolar spectrum³ consisting of a ¹³C-¹H Pake doublet, scaled by the WAHUA decoupling, and broken up into sidebands by the magic-angle spinning.⁷

Molecular motion modifies this pattern just as it does quadrupolar line shapes.^{1,3}

Carbon dipolar tensor simulations were performed by using the methods developed by Herzfeld and Berger.⁸ Calculations of tensors partially collapsed by restricted molecular motion were performed by assuming the motion was fast compared to the dipolar interactions. Formulas for tensor components under various types of restricted motions (and compatible with the Herzfeld and Berger analysis) are given in the appendix to ref 3.

Polycarbonate and tetrachloropolycarbonate were examined as annealed molded glasses, and the two PPOs as precipitated powders.

Conformational maps were calculated by modeling the benzene-benzene interaction potential using the Gaussian overlap procedure due to Berne and Pechukas.⁹ This model treats phenyl rings as ellipsoids of revolution. The potential is proportional to the amount of overlap of the ellipsoids, with bond-angle bending or stretching not included. The overlap model yields orientation-dependent range and strength parameters which are used in conjunction with a 12-6 Lennard-Jones potential. The overlap model thus reduces the calculation of the benzene-benzene interaction from a large sum of atomic site-site terms to a single two-body term with a distance and orientation dependence. The overlap model is also used for isotropic molecules, which are treated as spheres. In producing conformational maps for both polycarbonate and poly(phenylene oxide), oblate ellipsoids were used for the rings, and spheres for the methyl groups.

Results

Dipolar rotational spin-echo ¹³C NMR spectra of a methyl-brominated version of PPO are shown in Figure 1. The resonances of the protonated aromatic carbons (115 ppm) and the methylene carbons (25 ppm) rapidly dephase after as little as two WAHUA cycles. The nonprotonated aromatic-carbon signals (130-160 ppm) are not strongly influenced by proton coupling and experience little dephasing. The methyl-carbon signal (15 ppm) is intermediate in behavior.

All the carbon resonances refocus after 16 cycles. The rotation period for the magic-angle spinning was chosen

[†] Present address: Department of Macromolecular Science, Case Western Reserve University, Cleveland, OH 44106.

[‡] A. P. Sloan Foundation Fellow.